Letter

Kerr nonlinearity induced strong spin-magnon coupling

Feng-Zhou Ji and Jun-Hong An*

Key Laboratory of Quantum Theory and Applications of MoE, Lanzhou Center for Theoretical Physics, and Key Laboratory of Theoretical Physics of Gansu Province, Lanzhou University, Lanzhou 730000, China

(Received 13 August 2023; revised 5 November 2023; accepted 13 November 2023; published 27 November 2023)

One pillar of quantum magnonics is the exploration of the utilization of the mediation role of magnons in different platforms to develop quantum technologies. The efficient coupling between magnons and various quantum entities is a prerequisite. Here, we propose a scheme to enhance the spin-magnon coupling by the magnonic Kerr nonlinearity in a YIG sphere. We find that the Kerr-enhanced spin-magnon coupling invalidates the widely used single-Kittel-mode approximation to magnons. It is revealed that the spin decoherence induced by the multimode magnons in the strong-coupling regime becomes not severe, but suppressed, manifesting as either population trapping or persistent Rabi-like oscillation. This anomalous effect is because the spin changes to be so hybridized with the magnons that one or two bound states are formed between them. Enriching the spin-magnon coupling physics, the result supplies a guideline to control the spin-magnon interface.

DOI: 10.1103/PhysRevB.108.L180409

Introduction. Magnons are the elementary excitation of a collective spin wave in magnetic materials. The quantized interactions of magnons with different quantum platforms have inspired many novel applications in quantum technologies [1–11]. Besides quantum transduction [12], memory [13], sensing [14,15], and unidirectional invisibility [16], using the coupling between magnons and photons or phonons, the efficient couplings of magnons to spins have attracted much attention due to their potential realization of quantum networks [17] and quantum sensing [18–20]. The efficient spin-magnon couplings via either direct interactions [21–28] or the indirect way by exchanging photons or phonons [29–32] have been proposed. How to enhance the spin-magnon coupling strength is a prerequisite to explore their applications.

The Kerr nonlinearity of magnons in magnetic materials supplies a useful mechanism in quantum-state engineering [33,34]. Based on it, magnon-polariton bistability [35–37] and tristability [38,39], which are useful in the microwave nonreciprocal transmission [40], high-order sideband [41–43] and entanglement generations [44], and quantum phase transition [45], have been reported. A scheme to enhance the spin-magnon coupling using the Kerr nonlinearity was proposed in Ref. [46]. These works on quantum magnonics were generally based on an approximation in which the magnons are effectively treated as a single first-order Kittel mode [47–50]. It has been revealed that the higher-order magnonic modes are non-negligible in the presence of the Kerr nonlinearity [51–53]. References [23–25] studied the interactions between spins and multimode magnons. However, they are under the Markovian approximation, which is only valid in the weak-coupling condition.

Here, we investigate the non-Markovian dynamics of a spin defect coupled to magnons in a YIG sphere. A scheme to enhance the spin-magnon coupling by the magnonic Kerr nonlinearity is proposed. We find that the increasing of the coupling invalidates the widely used single-mode approximation of magnons to describe the matter-magnon coupling. The strong coupling also causes the spin to exhibit features with a suppressed decoherence, i.e., from the conventional oscillating damping to either the population trapping or the persistent Rabi-like oscillation. Our analysis reveals that such an anomalous decoherence is due to the formation of different numbers of spin-magnon bound states. Indicating that the Kerr nonlinearity endows the spin-magnon interface with a good controllability, our result paves the way to design quantum magnon devices.

System and spectral density. We consider a spin defect as a magnetic emitter coupled to the magnons attached to a YIG sphere in the presence of the Kerr nonlinearity (see Fig. 1). Its Hamiltonian reads [22,26]

$$\hat{\mathcal{H}}_{\text{Kerr}} = \hbar\omega_0\hat{\sigma}^\dagger\hat{\sigma} + \sum_k \big[\hbar\omega_k\hat{b}_k^\dagger\hat{b}_k - (\hbar K/2)\hat{b}_k^{\dagger 2}\hat{b}_k^2 - (g_k\hat{b}_k^\dagger\hat{\sigma} - \Omega_d e^{i\phi_d}\hat{b}_k^\dagger e^{-i\omega_d t} + \text{H.c.})\big]. \quad (1)$$

Here, $\hat{\sigma} = |g\rangle\langle e|$ is the transition operator of the spin defect with frequency ω_0 from the excited state $|e\rangle$ to the ground state $|g\rangle$, $\hat{b}_k$ is the annihilation operator of the kth magnon mode with frequency ω_k, and $g_k = \mu_0\mathbf{m}\cdot\tilde{\mathbf{H}}_k^*(\mathbf{r})$, with $\mathbf{m}$ being the spin magnetic moment and $\tilde{\mathbf{H}}_k(\mathbf{r})$ being the vacuum amplitude of the kth magnon mode concentrated around the YIG sphere, is their coupling strength. An inhomogeneous rf magnetic excited field is needed to trigger the multimode magnons [54]. The magnons are further driven by a microwave field with frequency ω_d, amplitude Ω_d, and phase ϕ_d. The Kerr nonlinearity quantified by K is caused by the magnetocrystalline anisotropy of the YIG sphere. It has been used to generate the magnon squeezing [34], which is attractive to the application of the magnons [1,55]. Rewriting the magnon operators as the sum of their steady-state mean value and fluctuations, i.e., $\hat{b}_k = \langle\hat{b}_k\rangle + \delta\hat{b}_k$, and neglecting the high-order

*anjhong@lzu.edu.cn

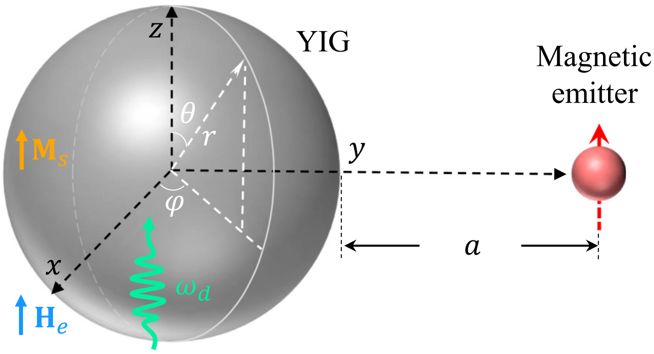

FIG. 1. Schematic illustration of the system. A magnetic emitter interacts with the magnons in a YIG sphere with radius R in a static magnetic field $\mathbf{H}_e$, and an induced magnetic field $\mathbf{M}_s$. A driving field with frequency ω_d is applied.

fluctuation terms in the strong driving condition, Eq. (1) in the rotating frame with $\hat{\mathcal{H}}_0=\omega_d(\hat{\sigma}^\dagger\hat{\sigma}+\sum_k\hat{b}_k^\dagger\hat{b}_k)$ becomes (see Supplemental Material [56])

$$\hat{\mathcal{H}}_{\text{Linear}}=\hbar\Delta_0\hat{\sigma}^\dagger\hat{\sigma}+\sum_k\big\{\hbar(\omega_k-\Pi_k)\hat{b}_k^\dagger\hat{b}_k-[g_k\hat{b}_k^\dagger\hat{\sigma}+(\hbar\mathcal{K}_k/2)\hat{b}_k^2+\text{H.c.}]\big\},\quad(2)$$

where $\Delta_0=\omega_0-\omega_d$, $\Pi_k=\omega_d+2\mathcal{K}_k$, and $\mathcal{K}_k=K\langle\hat{b}_k\rangle^2$. We have rewritten $\delta\hat{b}_k$ as $\hat{b}_k$ for brevity. Making the Bogoliubov transformation $\hat{\mathcal{S}}=\exp[\sum_k r_k(\hat{b}_k^2-\hat{b}_k^{\dagger 2})/2]$, with $r_k=\frac{1}{4}\ln(\frac{\omega_k-\Pi_k+\mathcal{K}_k}{\omega_k-\Pi_k-\mathcal{K}_k})$, to Eq. (2) and neglecting the counter-rotating terms [46], we obtain

$$\hat{\mathcal{H}}=\hbar\Delta_0\hat{\sigma}^\dagger\hat{\sigma}+\sum_k[\hbar\zeta_k\hat{b}_k^\dagger\hat{b}_k-(\mathcal{G}_k\hat{b}_k^\dagger\hat{\sigma}+\text{H.c.})],\quad(3)$$

where $\zeta_k=(\omega_k-\Pi_k)/\cosh(2r_k)$ and $\mathcal{G}_k=e^{r_k}g_k/2$. We find that the spin-magnon coupling is exponentially enhanced and the magnon frequencies are suppressed by the Kerr nonlinearity assisted by the microwave driving. This is one of our main results. To simplify our discussion, we approximate $\Pi_k\simeq\omega_d$ due to $\omega_d\gg\mathcal{K}_k$ and $r_k\equiv r$ by neglecting their k dependence, which is valid by properly choosing Ω_d and ω_d in our finite magnonic bandwidth case [54].

Consider that the YIG sphere is at low temperature such that the magnons are initially in the vacuum state [44,57]. After tracing over the magnonic degrees of freedom from the dynamics of the spin-magnon system, we derive an exact master equation of the spin as (see Supplemental Material [56])

$$\dot{\rho}(t)=i\Omega(t)[\rho(t),\hat{\sigma}^\dagger\hat{\sigma}]+\Gamma(t)[2\hat{\sigma}\rho(t)\hat{\sigma}^\dagger-\{\hat{\sigma}^\dagger\hat{\sigma},\rho(t)\}].\quad(4)$$

The renormalized frequency is $\Omega(t)=-\text{Im}[\dot{c}(t)/c(t)]$ and the decay rate is $\Gamma(t)=-\text{Re}[\dot{c}(t)/c(t)]$, where $c(t)$ satisfies

$$\dot{c}(t)+i\Delta_0c(t)+\int_0^t d\tau c(\tau)f(t-\tau)=0,\quad(5)$$

under $c(0)=1$. The convolution in Eq. (5) makes the dynamics non-Markovian with all the memory effects incorporated in the time-dependent coefficients in Eq. (4). The magnonic correlation function is $f(t-\tau)=\int_{\zeta_{\min}}^{\zeta_{\max}}d\zeta J(\zeta)e^{-i\zeta(t-\tau)}$ and the spectral density is [22]

$$J(\zeta)=\frac{\eta\mu_0}{4\hbar\pi}\text{Im}\{\mathbf{m}^*\cdot k^2\mathbf{G}[\mathbf{r},\mathbf{r},\zeta\cosh(2r)+\Pi]\cdot\mathbf{m}\},\quad(6)$$

where $k=[\zeta\cosh(2r)+\Pi]/c$ and $\eta=e^{2r}\cosh(2r)$. The Green's tensor reads $\bar{k}^2\mathbf{G}(\mathbf{r},\mathbf{a},\bar{\omega})=\sum_{\alpha,\beta\in\{r,\theta,\varphi\}}[H_{0,\alpha}^{\beta}+H_\alpha^\beta]\mathbf{e}_\alpha\mathbf{e}_\beta$, where $\mathbf{H}=-\nabla\phi$ and $\mathbf{H}_0$ takes the similar form as $\mathbf{H}$ but in the absence of the YIG sphere. The potential ϕ caused by the YIG satisfying $\phi=\frac{1}{4\pi}\nabla_a\frac{1}{|\mathbf{r}-\mathbf{a}|}$ is subject to the boundary condition of $(1+\chi)(\frac{\partial^2}{\partial x^2}+\frac{\partial^2}{\partial y^2})\phi+\frac{\partial^2\phi}{\partial z^2}=0$ in $r\leqslant R$ and $\nabla^2\phi=0$ in $r>R$ [58]. χ is the magnetic susceptibility tensor and determined by the Landau-Lifshitz-Gilbert equation as [59,60]

$$\chi_{xx}=\chi_{yy}=\frac{\gamma^2h_0M_s}{\gamma^2h_0^2-\omega^2-i\Gamma_0\omega}\equiv\chi,$$
$$\chi_{xy}=\chi_{yx}^*=i\frac{\gamma\omega M_s}{\gamma^2h_0^2-\omega^2-i\Gamma_0\omega}\equiv i\kappa,\quad(7)$$

where γ is the gyromagnetic ratio, $\Gamma_0=2\gamma h_0\alpha$, with α being the Gilbert parameter, is the damping parameter, $\mathbf{h}_0=h_0\mathbf{e}_z=\mathbf{H}_e+\mathbf{H}_d$, with $\mathbf{H}_e$ being the external static field and $\mathbf{H}_d=-\mathbf{M}_s/3$ being the demagnetization field, and $\mathbf{M}_s$ is the saturation magnetization. Putting the spin on the equatorial plane of the YIG sphere, i.e., $\theta=\pi/2$, and choosing $\mathbf{m}=-\mu_B(\mathbf{e}_x+i\mathbf{e}_y)=-\mu_Be^{i\varphi}(\mathbf{e}_r+i\mathbf{e}_\varphi)$, we have the nonzero components of the Green's tensor as $\text{Im}[\mathbf{m}^*\cdot\mathbf{G}\cdot\mathbf{m}]=\mu_B^2[\text{Im}(\mathbf{G}_{rr}+\mathbf{G}_{\varphi\varphi})+\text{Re}(\mathbf{G}_{r\varphi}-\mathbf{G}_{\varphi r})]$ [22,24,48]. The analytic form of $\mathbf{G}(\mathbf{r},\mathbf{a},\bar{\omega})$ is given in (see Supplemental Material [56]). The Green's tensor and the spectral density show resonance peaks determined by [59,60]

$$(n+1-m\kappa)P_n^m(\xi_0)+\xi_0P_n^{m\prime}(\xi_0)=0,\quad(8)$$

where P_n^m is the associated Legendre polynomial and $\xi_0=(1+1/\chi)^{1/2}$. The magnon modes corresponding to $n=-m=1$, 2, and 3 in the absence of the Kerr nonlinearity are the dipole or Kittel mode $\omega_\text{K}=\gamma(h_0+M_s/3)$, the quadrupolar mode $\omega_\text{Q}=\gamma(h_0+2M_s/5)$, and the octupolar mode $\omega_\text{O}=\gamma(h_0+3M_s/7)$, respectively. In the presence of the Kerr nonlinearity, they become $\zeta_{\text{K,Q,O}}=(\omega_{\text{K,Q,O}}-\Pi)/\cosh(2r)$. Ranging all m and n, it was found that the frequency range of $J(\zeta)$ is from $\zeta_{\min}=(\gamma h_0-\Pi)/\cosh(2r)$ to $\zeta_{\max}=[\gamma(h_0+M_s/2)-\Pi]/\cosh(2r)$ [54].

Spin dynamics. A widely used approximation in studying matter-magnon coupling is the Markovian approximation [23–25,47,50,61–63]. It is valid when their coupling is weak and the timescale of $f(t-\tau)$ is much smaller than the one of the matter. After replacing $c(\tau)$ by $c(t)$ and extending the upper bound of the time integral to infinity, the Markovian approximate solution of Eq. (5) is $c_{\text{MA}}(t)=e^{-[\Lambda+i\Upsilon(\Delta_0)]t}$, where $\Upsilon(\Delta_0)=\mathcal{P}\int d\zeta J(\zeta)/(\Delta_0-\zeta)$ is the Lamb shift and $\Lambda=\pi J(\Delta_0)$ is the spontaneous emission rate. The exponential-decay feature of $|c_{\text{MA}}(t)|^2$ characterizes a unidirectional energy flow from the spin to the magnons and the destructive effect of the magnons on the spin. This approximation cannot reflect the energy back flow induced by the strong spin-magnon coupling [22,26].

A pseudocavity method was proposed to study the strong light-matter coupling in an absorptive medium [64–68]. Keeping only the Kittel mode ζ_K, we approximate $J(\zeta)$ as a Lorentzian form $\mathcal{J}(\omega)=\frac{J(\zeta_K)(\gamma_p/2)^2}{(\omega-\zeta_K)^2+(\gamma_p/2)^2}$. The system is effectively seen as a spin coherently interacting with a pseudocavity mode $\hat{a}$ with frequency ζ_K and damping rate γ_p in a coupling strength $g^2=\pi J(\zeta_K)\gamma_p/2$. Here, γ_p is relevant to the damping parameter Γ_0. Thus, the spin dynamics is phenomenologically described by

$$\dot{\rho}(t)=i[\rho(t),\Delta_0\hat{\sigma}^\dagger\hat{\sigma}+\zeta_K\hat{a}^\dagger\hat{a}+g(\hat{a}\hat{\sigma}^\dagger+\text{H.c.})]+\frac{\gamma_p}{2}[2\hat{a}\rho(t)\hat{a}^\dagger-\{\hat{a}^\dagger\hat{a},\rho(t)\}]. \quad (9)$$

Although partially reflecting the energy backflow from the magnons to the spin, this method misses important physics from the magnonic higher-order resonant modes.

To fully capture the physics of the strong spin-magnon coupling enhanced by the Kerr nonlinearity and uncover the condition under which the pseudocavity method is applicable, we investigate the exact spin dynamics by choosing $\Delta_0=\zeta_K$. The steady-state solution of Eq. (5) is computable by a Laplace transform. It converts Eq. (5) into $\tilde{c}(s)=[s+i\Delta_0+\int_{\zeta_{\min}}^{\zeta_{\max}}d\zeta\frac{J(\zeta)}{s+i\zeta}]^{-1}$. $c(t)$ is obtained by making an inverse Laplace transform to $\tilde{c}(s)$, which requires finding its poles via (see Supplemental Material [56])

$$\frac{E}{\hbar}=\Delta_0+\int_{\zeta_{\min}}^{\zeta_{\max}}\frac{J(\zeta)}{E/\hbar-\zeta}d\zeta\equiv Y(E), \quad (10)$$

where $E=i\hbar s$. First, the roots E of Eq. (10) are exactly the eigenenergies of the total spin-magnon system. To prove this, we expand the eigenstate as $|\phi_E\rangle=x|e,\{0_k\}\rangle+\sum_k y_k|g,1_k\rangle$. Substituting $|\phi_E\rangle$ into $\hat{\mathcal{H}}|\phi_E\rangle=E|\phi_E\rangle$, we readily obtain Eq. (10). Second, because $Y(E)$ is a decreasing function in the regimes $E\in(-\infty,\hbar\zeta_{\min}]$ and $[\hbar\zeta_{\max},+\infty)$, Eq. (10) has one isolated root E^b in $(-\infty,\hbar\zeta_{\min}]$ or $[\zeta_{\max},+\infty)$ provided $Y(\hbar\zeta_{\min})<\hbar\zeta_{\min}$ or $Y(\hbar\zeta_{\max})>\hbar\zeta_{\max}$. The eigenstate corresponding to E^b is called the bound state. On the other hand, $Y(E)$ is nonanalytical in the regime $E\in[\hbar\zeta_{\min},\hbar\zeta_{\max}]$ due to the singularity in its integration. Therefore, Eq. (10) has an infinite number of roots in this regime, which form an energy band. Using the residue theorem, we have $c(t)=\sum_{j=1}^M Z_j e^{\frac{-i}{\hbar}E_j^b t}+\int_{\zeta_{\min}}^{\zeta_{\max}}\Theta(E)e^{-iEt}dE$, where $\Theta(E)=\frac{J(E)}{[E-\Delta_0-\Upsilon(E/\hbar)]^2+[\pi J(E)]^2}$, M being the number of the bound states, and $Z_j=[1+\int_{\zeta_{\min}}^{\zeta_{\max}}\frac{J(\zeta)d\zeta}{(E_j^b/\hbar-\zeta)^2}]^{-1}$ the residue contributed by the jth bound state. Oscillating with time in continuously changing frequencies $E/\hbar$ of the band energies, the integrand tends to zero in the long-time limit due to the out-of-phase interference. Thus, the steady-state solution of Eq. (10) is [69]

$$\lim_{t\to\infty}c(t)=\begin{cases}0, & \text{no bound state,}\\ \sum_{j=1}^M Z_j e^{\frac{-i}{\hbar}E_j^b t}, & M\text{ bound states.}\end{cases} \quad (11)$$

Assuming the spin is initially in $|e\rangle$ and solving Eq. (4), we obtained that the excited-state population is just $|c(t)|^2$ (see Supplemental Material [56]). Thus, Eq. (11) reveals that thanks to the Kerr-nonlinearity-enhanced spin-magnon coupling, the formation of the bound states would prevent the spin from relaxing to its ground state. Since it is not obtained from both the Markovian approximation and the pseudocavity method, such an anomalous decoherence manifests the distinguished role played by the non-Markovian effect and the feature of the energy spectrum of the total spin-magnon system in the decoherence of the spin. This is another main result of our work.

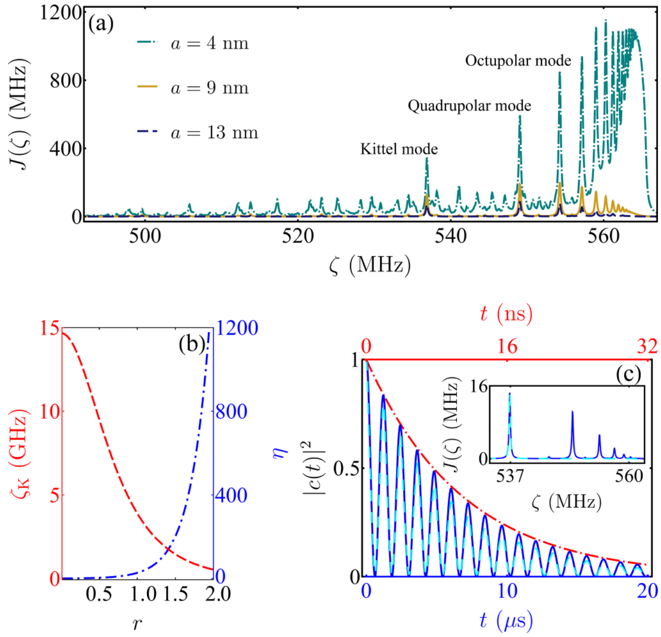

FIG. 2. (a) Spectral density $J(\zeta)$ in different spin-YIG distance a. (b) Kittel-mode frequency ζ_K and enhancement coefficient η in different r. (c) Evolution of the excited-state population $|c(t)|^2$ from the Markovian approximation (red dotted line), the pseudocavity method (cyan dashed line), and the non-Markovian dynamics (blue line). The inset is $J(\zeta)$ and the fitted Lorentzian form $\mathcal{J}(\zeta)$. We use $\omega_d=1$ GHz, $\gamma=28\,\text{GHz}\,\text{T}^{-1}$, $\Gamma_0=8\times10^{-3}$ GHz, $M_s=0.178$ T, $h_0=0.5$ T, $R=30$ nm, $r=2$ in (a) and (c), and $a=26$ nm in (c).

Numerical results. We plot in Fig. 2(a) the spectral density $J(\zeta)$ in different spin-YIG distance a for $r=2$. The driving-field frequency ω_d is chosen as $\omega_d=1$ GHz and the Kerr coefficient K relates to the volume V of the three-dimensional YIG sphere, i.e., $K\propto V^{-1}$ [34], and is about kHz [46], which makes the validity of $\Pi\simeq\omega_d$. We really see that $J(\zeta)$ exhibits obvious peaks at $\zeta=537$, 549, and 554 MHz irrespective of the value of a, which match well with our analytical frequencies $\zeta_{K,Q,O}$ of the Kittel, quadrupolar, and octupolar modes evaluated from Eq. (8). With decreasing a, $J(\zeta)$ shows an increase due to the near-field enhancement [26]. It signifies a strong spin-magnon coupling in the small-a regime. Figure 2(b) shows the effect of the Kerr nonlinearity on enhancing the spin-magnon coupling. It reveals that with increasing r from zero to 2, ζ_K decreases from 15 GHz to 537 MHz, while the prefactor η of $J(\zeta)$ increases from 1 to 1200. An efficient increase of about four orders of magnitude of η/ζ_K manifests a dramatic boost of the spin-magnon coupling strength. It confirms that the Kerr nonlinearity can be used to enhance the spin-magnon coupling [37,38,46].

Figure 2(c) shows the comparison of $|c(t)|^2$ obtained by three methods when $a=26$ nm. The exponential decay in

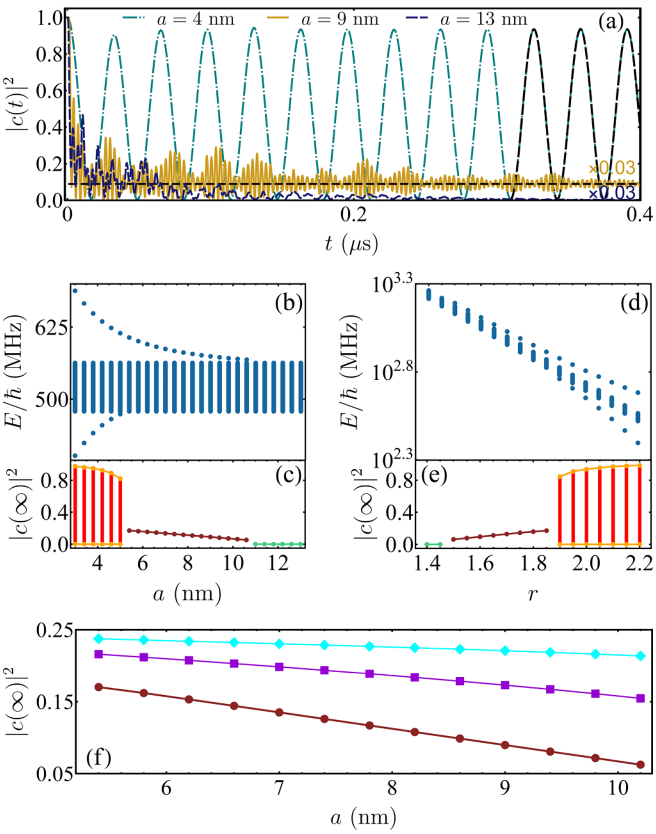

FIG. 3. (a) Evolution of $|c(t)|^2$ in different a. The black dashed lines are the corresponding steady-state values from Eq. (11). The time for the cases of $a = 9$ and 13 nm is magnified by a factor of 0.03. Energy spectrum of the whole system in different (b) a and (d) r obtained by solving Eq. (10). $|c(\infty)|^2$ from solving Eq. (5) denoted by the dots and from Eq. (11) denoted by the solid lines in different (c) a and (e) r. The red region covers the values during its persistent oscillation. (f) $|c(\infty)|^2$ when $\Delta_0 = \zeta_K$ (brown dot), ζ_Q (purple square), and ζ_O (cyan rhombus). $r = 2.0$ in (b) and (c), $a = 4$ nm in (d) and (e), and others are the same as Fig. 2(c).

the Markovian result entirely fails to describe the rapid spin-magnon energy exchanges obtained via numerically solving Eq. (5), which is fully captured by the pseudocavity method. It is the signature of the non-Markovian memory effect owned by the strong-coupling dynamics [70]. In this case, $J(\zeta)$ is dominated by the Kittel mode such that a Lorentzian fitting centered at ζ_K is sufficient and the pseudocavity method works well. However, with further decreasing a [see Fig. 2(a)] or increasing r, the high-order magnon modes become dominated, where the pseudocavity method no longer works.

Figure 3(a) shows the exact $|c(t)|^2$ in different a when $r = 2$. The strong spin-magnon coupling favored by both the near-field enhancement [26] and Kerr nonlinearity causes $|c(t)|^2$ to exhibit rich behaviors. It is interesting to find that in contrast to the damping to zero for $a = 13$ nm, which has no qualitative difference from the result predicted by the pseudocavity method, $|c(t)|^2$ approaches a finite value when $a = 9$ nm, while it exhibits a lossless Rabi-like oscillation when $a = 4$ nm. It reveals an anomalous behavior in which a small spin-magnon distance with the Kerr nonlinearity induces a strong spin-magnon coupling, which, on the contrary, causes a suppressed decoherence. It is not expected that a stronger spin-magnon coupling always causes a more severe decoherence to the spin [32,71]. This behavior can be explained by the features of the energy spectrum of the total spin-magnon system. Figure 3(b) indicates that two branches of bound states separate the energy spectrum into three regimes. When $a \geqslant 10.4$ nm, no bound state is formed and thus $|c(t)|^2$ decays to zero. When $4.8 < a < 10.4$ nm, one bound state is present and $|c(t)|^2$ tends to finite values. When $a \leqslant 4.8$ nm, two bound states are present and $|c(t)|^2$ behaves as a persistent Rabi-like oscillation in a frequency $|E_1^{\mathrm{b}} - E_2^{\mathrm{b}}|/\hbar$. The matching of the long-time behaviors of the three regimes with the analytical result in Eq. (11) verifies the distinguished role played by the bound states and non-Markovian effect in determining the strong-coupled spin-magnon physics; see Fig. 3(c). Figures 3(d) and 3(e) indicate that it is just the Kerr-nonlinearity-induced strong spin-magnon coupling that causes the formation of the bound states and the accompanying population trapping and persistent Rabi-like oscillation. Figure 3(f) shows $|c(\infty)|^2$ in the distances a supporting the formation of one bound state. It demonstrates that the trapped population $|c(\infty)|^2$ can be controlled by choosing Δ_0 as different magnonic resonant frequencies. All the results prove that the strong spin-magnon coupling endows the spin with rich anomalous decoherence governed by the formation of different numbers of bound states. It supplies a guideline to control the spin coherence via engineering the feature of the spin-magnon energy spectrum.

Discussion and conclusions. Quantum magnonics exploring the efficient couplings between magnons and different kinds of quantum matter has made great progress [1,4,19,31,32,35,37,72–76]. Many of these works were based on the single-magnon-mode approximation, which may be insufficient in the strong matter-magnon coupling. The coupling between single spins and multimode magnons was studied in Ref. [22], but the Kerr nonlinearity was absent. The Kerr nonlinearity has been observed in cavity magnon mechanics formed by the YIG [35,37,75]. The bound state and its distinguished role in the non-Markovian dynamics have been experimentally observed in both photonic crystal [77] and ultracold-atom [78,79] systems. The progress gives strong support that our finding is realizable in state-of-the-art experiments [76,80]. Note that although only the YIG is studied, our results are applicable to other magnetic materials, such as CoFeB [19,81]. As a final remark, the expectation value of the magnonic fluctuation operator described by $\hat{b}_k$ in Eq. (3) should be zero to ensure the self-consistence of our linearization approximation to Eq. (1). This can be proven as follows. The evolved state of the spin-magnon system under our studied initial condition $|\Psi_{\mathrm{tot}}(0)\rangle = |e, \{0_k\}\rangle$ reads $|\Psi_{\mathrm{tot}}(t)\rangle = c(t)|e, \{0_k\}\rangle + \sum_k d_k(t)|g, 1_k\rangle$, which readily leads to $\langle\Psi_{\mathrm{tot}}(t)|\hat{b}_k|\Psi_{\mathrm{tot}}(t)\rangle = 0$.

In summary, we have investigated the near-field interactions between a spin defect and magnons in a YIG sphere with Kerr nonlinearity. It is found that the Kerr nonlinearity induces a dramatic enhancement to the spin-magnon coupling. Contrary to the belief that a strong coupling always causes a severe decoherence, such a strong coupling makes the magnon-induced decoherence to the spin change from complete damping to either population trapping or persistent Rabi-like oscillation. This anomalous decoherence is due to the formation of different numbers of spin-magnon bound states. Breaking the dissipation barrier of the spin, our finding supplies a guideline to suppress the spin decoherence and design quantum magnonic devices.

Acknowledgments. This work is supported by the National Natural Science Foundation of China (Grants No. 12275109, No. 11834005, and No. 12247101) and the Supercomputing Center of Lanzhou University.

[1] H. Yuan, Y. Cao, A. Kamra, R. A. Duine, and P. Yan, Quantum magnonics: When magnon spintronics meets quantum information science, Phys. Rep. **965**, 1 (2022).

[2] D. Lachance-Quirion, Y. Tabuchi, A. Gloppe, K. Usami, and Y. Nakamura, Hybrid quantum systems based on magnonics, Appl. Phys. Express **12**, 070101 (2019).

[3] B. Zare Rameshti, S. Viola Kusminskiy, J. A. Haigh, K. Usami, D. Lachance-Quirion, Y. Nakamura, C.-M. Hu, H. X. Tang, G. E. Bauer, and Y. M. Blanter, Cavity magnonics, Phys. Rep. **979**, 1 (2022).

[4] X. Zhang, C.-L. Zou, L. Jiang, and H. X. Tang, Cavity magnomechanics, Sci. Adv. **2**, e1501286 (2016).

[5] A. V. Chumak, A. A. Serga, and B. Hillebrands, Magnon transistor for all-magnon data processing, Nat. Commun. **5**, 4700 (2014).

[6] Y. Nambu, J. Barker, Y. Okino, T. Kikkawa, Y. Shiomi, M. Enderle, T. Weber, B. Winn, M. Graves-Brook, J. M. Tranquada, T. Ziman, M. Fujita, G. E. W. Bauer, E. Saitoh, and K. Kakurai, Observation of magnon polarization, Phys. Rev. Lett. **125**, 027201 (2020).

[7] F.-X. Sun, S.-S. Zheng, Y. Xiao, Q. Gong, Q. He, and K. Xia, Remote generation of magnon Schrödinger cat state via magnon-photon entanglement, Phys. Rev. Lett. **127**, 087203 (2021).

[8] H. Y. Yuan, P. Yan, S. Zheng, Q. Y. He, K. Xia, and M.-H. Yung, Steady Bell state generation via magnon-photon coupling, Phys. Rev. Lett. **124**, 053602 (2020).

[9] J. Prokop, W. X. Tang, Y. Zhang, I. Tudosa, T. R. F. Peixoto, K. Zakeri, and J. Kirschner, Magnons in a ferromagnetic monolayer, Phys. Rev. Lett. **102**, 177206 (2009).

[10] Z.-Q. Wang, Y.-P. Wang, J. Yao, R.-C. Shen, W.-J. Wu, J. Qian, J. Li, S.-Y. Zhu, and J. Q. You, Giant spin ensembles in waveguide magnonics, Nat. Commun. **13**, 7580 (2022).

[11] Z. Li, M. Ma, Z. Chen, K. Xie, and F. Ma, Interaction between magnon and skyrmion: Toward quantum magnonics, J. Appl. Phys. **132**, 210702 (2022).

[12] R. Hisatomi, A. Osada, Y. Tabuchi, T. Ishikawa, A. Noguchi, R. Yamazaki, K. Usami, and Y. Nakamura, Bidirectional conversion between microwave and light via ferromagnetic magnons, Phys. Rev. B **93**, 174427 (2016).

[13] X. Zhang, C.-L. Zou, N. Zhu, F. Marquardt, L. Jiang, and H. X. Tang, Magnon dark modes and gradient memory, Nat. Commun. **6**, 8914 (2015).

[14] C. A. Potts, V. A. S. V. Bittencourt, S. V. Kusminskiy, and J. P. Davis, Magnon-phonon quantum correlation thermometry, Phys. Rev. Appl. **13**, 064001 (2020).

[15] N. Crescini, C. Braggio, G. Carugno, A. Ortolan, and G. Ruoso, Cavity magnon polariton based precision magnetometry, Appl. Phys. Lett. **117**, 144001 (2020).

[16] Y.-P. Wang, J. W. Rao, Y. Yang, P.-C. Xu, Y. S. Gui, B. M. Yao, J. Q. You, and C.-M. Hu, Nonreciprocity and unidirectional invisibility in cavity magnonics, Phys. Rev. Lett. **123**, 127202 (2019).

[17] C. C. Rusconi, M. J. A. Schuetz, J. Gieseler, M. D. Lukin, and O. Romero-Isart, Hybrid architecture for engineering magnonic quantum networks, Phys. Rev. A **100**, 022343 (2019).

[18] D. Lachance-Quirion, S. P. Wolski, Y. Tabuchi, S. Kono, K. Usami, and Y. Nakamura, Entanglement-based single-shot detection of a single magnon with a superconducting qubit, Science **367**, 425 (2020).

[19] A. B. Solanki, S. I. Bogdanov, M. M. Rahman, A. Rustagi, N. R. Dilley, T. Shen, W. Tong, P. Debashis, Z. Chen, J. Appenzeller, Y. P. Chen, V. M. Shalaev, and P. Upadhyaya, Electric field control of interaction between magnons and quantum spin defects, Phys. Rev. Res. **4**, L012025 (2022).

[20] D. Prananto, Y. Kainuma, K. Hayashi, N. Mizuochi, K.-I. Uchida, and T. An, Probing thermal magnon current mediated by coherent magnon via nitrogen-vacancy centers in diamond, Phys. Rev. Appl. **16**, 064058 (2021).

[21] Y. Tabuchi, S. Ishino, A. Noguchi, T. Ishikawa, R. Yamazaki, K. Usami, and Y. Nakamura, Coherent coupling between a ferromagnetic magnon and a superconducting qubit, Science **349**, 405 (2015).

[22] T. Neuman, D. S. Wang, and P. Narang, Nanomagnonic cavities for strong spin-magnon coupling and magnon-mediated spin-spin interactions, Phys. Rev. Lett. **125**, 247702 (2020).

[23] M. Fukami, D. R. Candido, D. D. Awschalom, and M. E. Flatté, Opportunities for long-range magnon-mediated entanglement of spin qubits via on- and off-resonant coupling, PRX Quantum **2**, 040314 (2021).

[24] C. Gonzalez-Ballestero, T. van der Sar, and O. Romero-Isart, Towards a quantum interface between spin waves and paramagnetic spin baths, Phys. Rev. B **105**, 075410 (2022).

[25] K. Ullah, E. Köse, R. Yagan, M. C. Onbaşlı, and Ö. E. Müstecaplıoğlu, Steady state entanglement of distant nitrogen-vacancy centers in a coherent thermal magnon bath, Phys. Rev. Res. **4**, 023221 (2022).

[26] V. Karanikolas, T. Kuroda, and J. I. Inoue, Magnon-mediated spin entanglement in the strong-coupling regime, Phys. Rev. Res. **4**, 043180 (2022).

[27] K. An, R. Kohno, A. N. Litvinenko, R. L. Seeger, V. V. Naletov, L. Vila, G. de Loubens, J. Ben Youssef, N. Vukadinovic, G. E. W. Bauer, A. N. Slavin, V. S. Tiberkevich, and O. Klein, Bright and dark states of two distant macrospins strongly coupled by phonons, Phys. Rev. X **12**, 011060 (2022).

[28] M. Kounalakis, G. E. W. Bauer, and Y. M. Blanter, Analog quantum control of magnonic cat states on a chip by a superconducting qubit, Phys. Rev. Lett. **129**, 037205 (2022).

[29] K. Wu, W.-X. Zhong, G.-L. Cheng, and A.-X. Chen, Phase-controlled multimagnon blockade and magnon-induced tunneling in a hybrid superconducting system, Phys. Rev. A **103**, 052411 (2021).

[30] Z.-X. Liu, H. Xiong, M.-Y. Wu, and Y.-Q. Li, Absorption of magnons in dispersively coupled hybrid quantum systems, Phys. Rev. A **103**, 063702 (2021).
[31] W. Xiong, M. Wang, G.-Q. Zhang, and J. Chen, Optomechanical-interface-induced strong spin-magnon coupling, Phys. Rev. A **107**, 033516 (2023).
[32] X.-L. Hei, P.-B. Li, X.-F. Pan, and F. Nori, Enhanced tripartite interactions in spin-magnon-mechanical hybrid systems, Phys. Rev. Lett. **130**, 073602 (2023).
[33] M. Moslehi, H. R. Baghshahi, M. J. Faghihi, and S. Y. Mirafzali, Nonclassicality of dissipative cavity optomagnonics in the presence of Kerr nonlinearities, Phys. Scr. **98**, 025103 (2023).
[34] G. Zhang, Y. Wang, and J. You, Theory of the magnon Kerr effect in cavity magnonics, Sci. China Phys. Mech. Astron. **62**, 987511 (2019).
[35] Y.-P. Wang, G.-Q. Zhang, D. Zhang, T.-F. Li, C.-M. Hu, and J. Q. You, Bistability of cavity magnon polaritons, Phys. Rev. Lett. **120**, 057202 (2018).
[36] Z.-B. Yang, H. Jin, J.-W. Jin, J.-Y. Liu, H.-Y. Liu, and R.-C. Yang, Bistability of squeezing and entanglement in cavity magnonics, Phys. Rev. Res. **3**, 023126 (2021).
[37] R.-C. Shen, J. Li, Z.-Y. Fan, Y.-P. Wang, and J. Q. You, Mechanical bistability in Kerr-modified cavity magnomechanics, Phys. Rev. Lett. **129**, 123601 (2022).
[38] R.-C. Shen, Y.-P. Wang, J. Li, S.-Y. Zhu, G. S. Agarwal, and J. Q. You, Long-time memory and ternary logic gate using a multistable cavity magnonic system, Phys. Rev. Lett. **127**, 183202 (2021).
[39] M. X. Bi, X. H. Yan, Y. Zhang, and Y. Xiao, Tristability of cavity magnon polaritons, Phys. Rev. B **103**, 104411 (2021).
[40] C. Kong, H. Xiong, and Y. Wu, Magnon-induced nonreciprocity based on the magnon Kerr effect, Phys. Rev. Appl. **12**, 034001 (2019).
[41] Z.-X. Liu, B. Wang, H. Xiong, and Y. Wu, Magnon-induced high-order sideband generation, Opt. Lett. **43**, 3698 (2018).
[42] M. Wang, C. Kong, Z.-Y. Sun, D. Zhang, Y.-Y. Wu, and L.-L. Zheng, Nonreciprocal high-order sidebands induced by magnon Kerr nonlinearity, Phys. Rev. A **104**, 033708 (2021).
[43] C. Zhao, Z. Yang, R. Peng, J. Yang, C. Li, and L. Zhou, Dissipative-coupling-induced transparency and high-order sidebands with Kerr nonlinearity in a cavity-magnonics system, Phys. Rev. Appl. **18**, 044074 (2022).
[44] Z. Zhang, M. O. Scully, and G. S. Agarwal, Quantum entanglement between two magnon modes via Kerr nonlinearity driven far from equilibrium, Phys. Rev. Res. **1**, 023021 (2019).
[45] Y. Qin, S.-C. Li, K. Li, and J.-J. Song, Controllable quantum phase transition in a double-cavity magnonic system, Phys. Rev. B **106**, 054419 (2022).
[46] W. Xiong, M. Tian, G.-Q. Zhang, and J. Q. You, Strong long-range spin-spin coupling via a Kerr magnon interface, Phys. Rev. B **105**, 245310 (2022).
[47] J. Li, S.-Y. Zhu, and G. S. Agarwal, Magnon-photon-phonon entanglement in cavity magnomechanics, Phys. Rev. Lett. **121**, 203601 (2018).
[48] K. An, A. N. Litvinenko, R. Kohno, A. A. Fuad, V. V. Naletov, L. Vila, U. Ebels, G. de Loubens, H. Hurdequint, N. Beaulieu, J. Ben Youssef, N. Vukadinovic, G. E. W. Bauer, A. N. Slavin, V. S. Tiberkevich, and O. Klein, Coherent long-range transfer of angular momentum between magnon Kittel modes by phonons, Phys. Rev. B **101**, 060407(R) (2020).
[49] S.-F. Qi and J. Jing, Magnon-mediated quantum battery under systematic errors, Phys. Rev. A **104**, 032606 (2021).
[50] Y.-l. Ren, J.-k. Xie, X.-k. Li, S.-l. Ma, and F.-l. Li, Long-range generation of a magnon-magnon entangled state, Phys. Rev. B **105**, 094422 (2022).
[51] R. G. E. Morris, A. F. van Loo, S. Kosen, and A. D. Karenowska, Strong coupling of magnons in a YIG sphere to photons in a planar superconducting resonator in the quantum limit, Sci. Rep. **7**, 11511 (2017).
[52] J. W. Rao, B. Yao, C. Y. Wang, C. Zhang, T. Yu, and W. Lu, Unveiling a pump-induced magnon mode via its strong interaction with Walker modes, Phys. Rev. Lett. **130**, 046705 (2023).
[53] V. A. S. V. Bittencourt, C. A. Potts, Y. Huang, J. P. Davis, and S. Viola Kusminskiy, Magnomechanical backaction corrections due to coupling to higher-order walker modes and Kerr nonlinearities, Phys. Rev. B **107**, 144411 (2023).
[54] L. R. Walker, Resonant modes of ferromagnetic spheroids, J. Appl. Phys. **29**, 318 (1958).
[55] M. Elyasi, Y. M. Blanter, and G. E. W. Bauer, Resources of nonlinear cavity magnonics for quantum information, Phys. Rev. B **101**, 054402 (2020).
[56] See Supplemental Material at http://link.aps.org/supplemental/10.1103/PhysRevB.108.L180409 for a detailed derivation of the linearized Hamiltonian, the magnetostatic Green's tensor, the spectral density, the energy spectrum, and the exact master equation of the spin system and its steady-state solution.
[57] N. Crescini, C. Braggio, G. Carugno, A. Ortolan, and G. Ruoso, Coherent coupling between multiple ferrimagnetic spheres and a microwave cavity at millikelvin temperatures, Phys. Rev. B **104**, 064426 (2021).
[58] D. L. Mills and E. Burstein, Polaritons: The electromagnetic modes of media, Rep. Prog. Phys. **37**, 817 (1974).
[59] L. R. Walker, Magnetostatic modes in ferromagnetic resonance, Phys. Rev. **105**, 390 (1957).
[60] P. C. Fletcher and R. O. Bell, Ferrimagnetic resonance modes in spheres, J. Appl. Phys. **30**, 687 (1959).
[61] G. Zhao, Y. Wang, and X.-F. Qian, Driven dissipative quantum dynamics in a cavity magnon-polariton system, Phys. Rev. B **104**, 134423 (2021).
[62] J. M. P. Nair, D. Mukhopadhyay, and G. S. Agarwal, Ultralow threshold bistability and generation of long-lived mode in a dissipatively coupled nonlinear system: Application to magnonics, Phys. Rev. B **103**, 224401 (2021).
[63] G.-Q. Zhang, Z. Chen, W. Xiong, C.-H. Lam, and J. Q. You, Parity-symmetry-breaking quantum phase transition via parametric drive in a cavity magnonic system, Phys. Rev. B **104**, 064423 (2021).
[64] A. Delga, J. Feist, J. Bravo-Abad, and F. J. Garcia-Vidal, Quantum emitters near a metal nanoparticle: Strong coupling and quenching, Phys. Rev. Lett. **112**, 253601 (2014).
[65] A. González-Tudela, P. A. Huidobro, L. Martín-Moreno, C. Tejedor, and F. J. García-Vidal, Reversible dynamics of single quantum emitters near metal-dielectric interfaces, Phys. Rev. B **89**, 041402(R) (2014).
[66] C.-J. Yang and J.-H. An, Suppressed dissipation of a quantum emitter coupled to surface plasmon polaritons, Phys. Rev. B **95**, 161408(R) (2017).

[67] D. Tamascelli, A. Smirne, S. F. Huelga, and M. B. Plenio, Nonperturbative treatment of non-Markovian dynamics of open quantum systems, Phys. Rev. Lett. **120**, 030402 (2018).

[68] I. Medina, F. J. García-Vidal, A. I. Fernández-Domínguez, and J. Feist, Few-mode field quantization of arbitrary electromagnetic spectral densities, Phys. Rev. Lett. **126**, 093601 (2021).

[69] F.-Z. Ji, S.-Y. Bai, and J.-H. An, Strong coupling of quantum emitters and the exciton polariton in MoS_2 nanodisks, Phys. Rev. B **106**, 115427 (2022).

[70] D. G. Baranov, M. Wersäll, J. Cuadra, T. J. Antosiewicz, and T. Shegai, Novel nanostructures and materials for strong light-matter interactions, ACS Photon. **5**, 24 (2018).

[71] J. Sloan, N. Rivera, J. D. Joannopoulos, I. Kaminer, and M. Soljačić, Controlling spins with surface magnon polaritons, Phys. Rev. B **100**, 235453 (2019).

[72] Y. Tabuchi, S. Ishino, T. Ishikawa, R. Yamazaki, K. Usami, and Y. Nakamura, Hybridizing ferromagnetic magnons and microwave photons in the quantum limit, Phys. Rev. Lett. **113**, 083603 (2014).

[73] D. Zhang, X.-Q. Luo, Y.-P. Wang, T.-F. Li, and J. Q. You, Observation of the exceptional point in cavity magnon-polaritons, Nat. Commun. **8**, 1368 (2017).

[74] H. Huebl, C. W. Zollitsch, J. Lotze, F. Hocke, M. Greifenstein, A. Marx, R. Gross, and S. T. B. Goennenwein, High cooperativity in coupled microwave resonator ferrimagnetic insulator hybrids, Phys. Rev. Lett. **111**, 127003 (2013).

[75] Y.-P. Wang, G.-Q. Zhang, D. Zhang, X.-Q. Luo, W. Xiong, S.-P. Wang, T.-F. Li, C.-M. Hu, and J. Q. You, Magnon Kerr effect in a strongly coupled cavity-magnon system, Phys. Rev. B **94**, 224410 (2016).

[76] Y. Li, V. G. Yefremenko, M. Lisovenko, C. Trevillian, T. Polakovic, T. W. Cecil, P. S. Barry, J. Pearson, R. Divan, V. Tyberkevych, C. L. Chang, U. Welp, W.-K. Kwok, and V. Novosad, Coherent coupling of two remote magnonic resonators mediated by superconducting circuits, Phys. Rev. Lett. **128**, 047701 (2022).

[77] Y. Liu and A. A. Houck, Quantum electrodynamics near a photonic band gap, Nat. Phys. **13**, 48 (2017).

[78] L. Krinner, M. Stewart, A. Pazmiño, J. Kwon, and D. Schneble, Spontaneous emission of matter waves from a tunable open quantum system, Nature (London) **559**, 589 (2018).

[79] J. Kwon, Y. Kim, A. Lanuza, and D. Schneble, Formation of matter-wave polaritons in an optical lattice, Nat. Phys. **18**, 657 (2022).

[80] S. Martínez-Losa del Rincón, I. Gimeno, J. Pérez-Bailón, V. Rollano, F. Luis, D. Zueco, and M. J. Martínez-Pérez, Measuring the magnon-photon coupling in shaped ferromagnets: Tuning of the resonance frequency, Phys. Rev. Appl. **19**, 014002 (2023).

[81] K. S. U. Kansanen, C. Tassi, H. Mishra, M. A. Sillanpää, and T. T. Heikkilä, Magnomechanics in suspended magnetic beams, Phys. Rev. B **104**, 214416 (2021).